Synthesis of Nitrogen-Doped Graphene Using Embedded Carbon and Nitrogen Sources

ARTICLE *in* ADVANCED MATERIALS · FEBRUARY 2011

Impact Factor: 17.49 · DOI: 10.1002/adma.201004110 · Source: PubMed

Synthesis of Nitrogen-Doped Graphene Using Embedded Carbon and Nitrogen Sources

*Chaohua Zhang, Lei Fu, Nan Liu, Minhao Liu, Yayu Wang, and Zhongfan Liu**

Graphene is the two-dimensional crystalline form of carbon whose extraordinary charge carrier mobility and other unique features hold great promise for nanoscale electronics.[1] Because graphene has no bandgap, however, its electrical conductivity cannot be completely controlled like classical semiconductor. Theoretical and experimental studies on graphene doping show the possibility of opening the bandgap and modulating conducting types by substituting carbon atoms with foreign atoms.[2] Graphene is easily p-doped by adsorbates like physisorbed oxygen molecules, but complementary doping (both n-type and p-type doping) is essential for functional device applications like complementary metal-oxide-semiconductor (CMOS) circuits.[3] Recently, a number of approaches have been proposed to synthesize nitrogen-doped graphene (NG), such as chemical vapor deposition (CVD),[2a,4] arc-discharge,[2b,5] and post treatments.[6] Here, we report a new approach which makes use of embedded nitrogen and carbon atoms in metal substrate to prepare NG. As doping is accompanied with the combination of carbon atoms into graphene during annealing process, N atoms can be substitutionally doped into the graphene lattice. Our method provides not only a better control over the doping density but also a potential advantage to precisely control the solid dopants at desired locations to achieve patterned doping.

Our approach for NG synthesis is actually the enthusiastic utilization of the very common segregation phenomenon to turn the trace amount of carbon and nitrogen dissolved in bulk metals into NG.[7] Metals usually contain a trace amount of carbon impurities, which could be brought into evaporated metal film during the electron beam deposition process.[7a,8] The clue of embedding nitrogen atoms into metal film comes from H. Konno et al.'s work in 1999.[9] In the boron-doping experiments of graphite, they always observed a simultaneous incorporation of nitrogen together with boron at high temperature, suggesting the efficient nitrogen fixation effect of boron species. This indicates that one can obtain nitrogen-embedded metal films with the aid of boron mediator during the electron beam deposition process. What's more, based on theoretical calculations,[10] boron atoms prefer to stay in the bulk of nickel, whereas nitrogen atoms tend to segregate out onto nickel surface. As shown in **Scheme 1**, our NG is synthesized through vacuum annealing a sandwiched Ni(C)/B(N)/SiO_2/Si substrate at high temperature. The boron and nickel layers were sequentially deposited on SiO_2/Si substrate by electron beam evaporation, where a trace amount of nitrogen species were incorporated into the boron layer spontaneously (Figure S1). During the vacuum annealing process, both boron-trapped nitrogen and nickel-trapped carbon atoms diffuse towards nickel surface and get segregated into NG. Actually, boron film performs a perfect nitrogen source carrier without introducing detectable boron atoms into the graphene, confirmed by X-ray photoelectron spectroscopy (XPS) (**Figure 1**a, S2). Pristine graphene (PG) is synthesized similarly by vacuum annealing a sandwiched Ni(C)/SiO_2/Si substrate. After growth, using our transfer-printing method,[11] PG and NG can be easily isolated from growth substrates and transferred to target substrates for further characterization.

Figure 1a shows the typical XPS results of NG and PG on nickel surface after growth. The NG sample shows an obvious N1s peak whereas there are no detectable N peaks in PG sample. The N1s peak in NG has three components centered at 398.2 eV, 400.3 eV and 401.5 eV, corresponding to pyridinic-N, pyrrolic-N, and graphitic-N,[2a,12] respectively (Figure 1b, d). Pyridinic- and pyrrolic-N are dominant in our NG samples, consistent with theoretical prediction that N atoms are more thermodynamically stable at the edges of graphene lattice.[6a] As shown in Figure 1c, the C1s peak of PG is located at 284.8 eV, corresponding to the graphite-like sp^2 C; while for NG, small peaks at 285.9 eV and 287.1 eV are clearly visualized in addition to the main sp^2 C peak, reflecting two different bonds, corresponding to the N-sp^2 C and N-sp^3 C, respectively, originating from the substitutional doping of N atoms.[2a] The C1s peak at 289.0 eV is attributed to CO type bond.[12a] The O1s peak is observed in both NG and PG samples, which is possibly due to physisorbed oxygen on the graphene surface. The higher peak intensity ratio of O1s to C1s in NG suggests stronger oxygen adsorption ability on NG surface, which may suggest a potential application in fuel cells.[4a] As nitrogen source is supplied by the evaporated boron films, the N content in the NG can be controlled by the relative thickness between boron and nickel films (Figure S3). Typically, the N/C atomic ratios in our NG, estimated by XPS, range from 0.3 to 2.9%. After transferring

C. H. Zhang,[+] Prof. L. Fu,[+] N. Liu, Prof. Z. F. Liu
Center for Nanochemistry
Beijing National Laboratory for Molecular Sciences
State Key Laboratory for Structural Chemistry of Unstable and Stable Species
College of Chemistry and Molecular Engineering
Academy for Advanced Interdisciplinary Studies
Peking University
Beijing, 100871, P. R. China
E-mail: zfliu@pku.edu.cn
M. H. Liu, Prof. Y. Y. Wang
Department of Physics
Tsinghua University
Beijing, 100084, P. R. China
[+] These authors contributed equally to this work.

DOI: 10.1002/adma.201004110

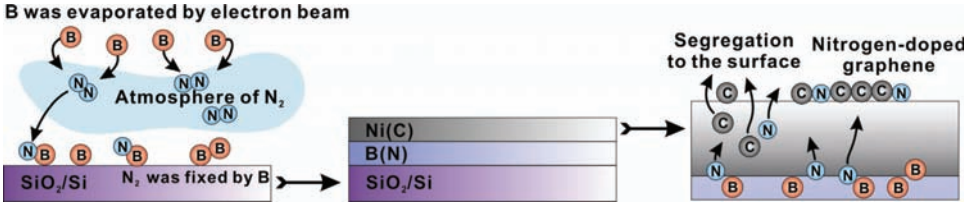

Scheme 1. Schematic illustration of our concurrent segregation technique for growing nitrogen-doped graphene. The electron beam evaporated boron layer was used as the nitrogen trap and the top nickel layer containing a trace amount of carbon as the segregation medium and carbon source. Nitrogen-doped graphene was formed on nickel surface after vacuum annealing at high temperature.

from growth substrate to SiO_2/Si substrate, we also detected an obvious N1s peak in NG sample (Figure S2).

Figure 2a shows the typical optical micrograph (OM) of NG transferred on 300 nm-thick SiO_2/Si surface. Similar to PG (Figure S4), NG is a large-area, continuous and uniform film. Layers of graphene can be verified by color contrast due to light interference effect.[1a] The regions with the same color are up to 90% over the entire substrate. Although there are sporadic multilayers in NG, the atomic force microscopy (AFM) image demonstrates that NG is uniform with an apparent thickness of about 1.1 nm (Figure 2b), suggesting NG is a few-layer film.[1a]

Raman spectroscopy is an effective tool to detect the doping effect of graphene. **Figure 3** compares the Raman spectra of PG, NG1 (N/C = 0.6 at.%) and NG2 (N/C = 2.9 at.%), which are taken from few-layer regions of the three samples. For PG, the D peak is barely seen, indicative of the absence of significant defects. As nitrogen atoms are doped into the graphene network, the D peak intensity rises rapidly. As demonstrated in the schematic structure of NG (Figure 1d), defects may include bonding disorders and vacancies in graphene lattice induced by nitrogen doping. On doping, the intensity of 2D peak decreases with respect

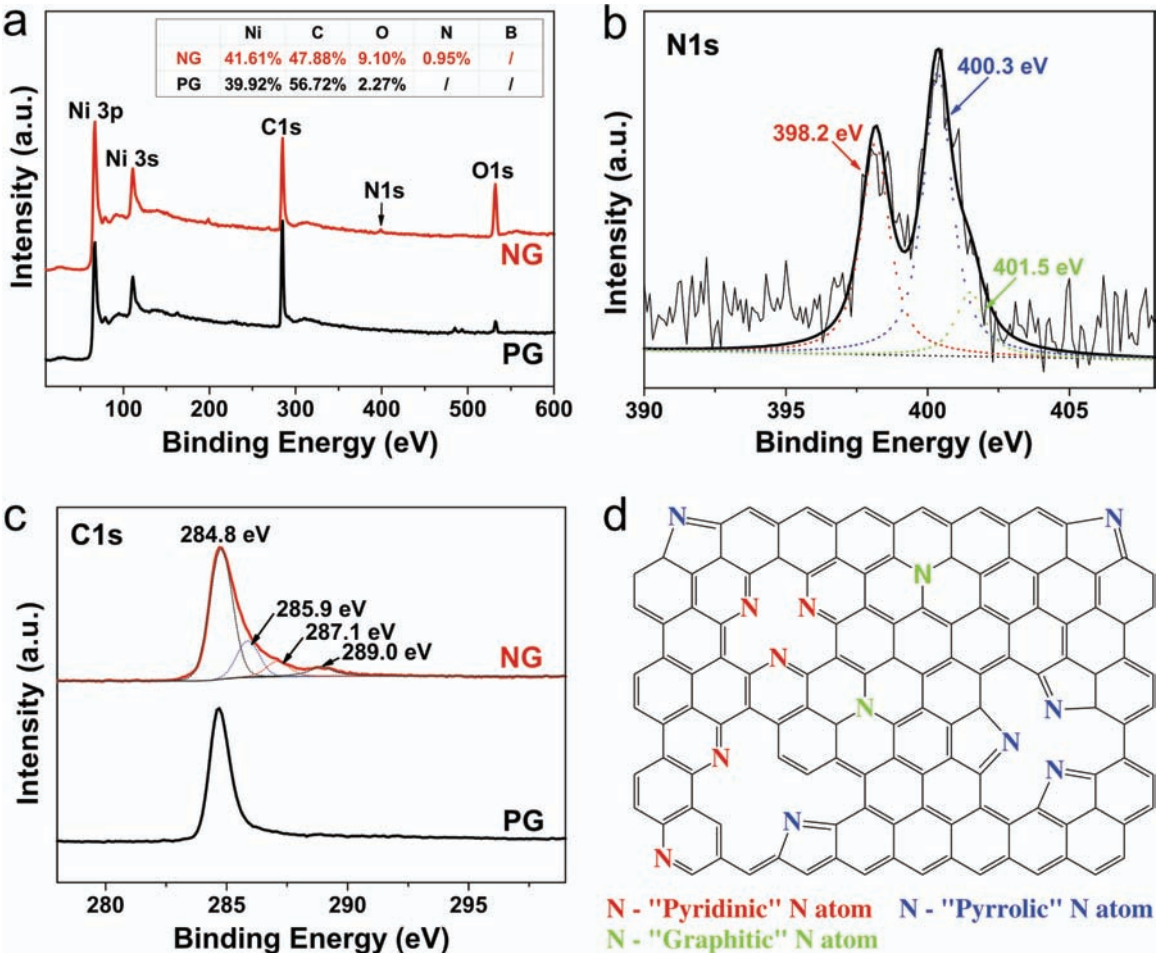

Figure 1. (a) XPS spectra of nitrogen-doped graphene (NG) and pristine graphene (PG) on nickel surface after growth. (b) N1s peak of NG. (c) C1s peaks of NG and PG. (d) Schematic structure of NG.

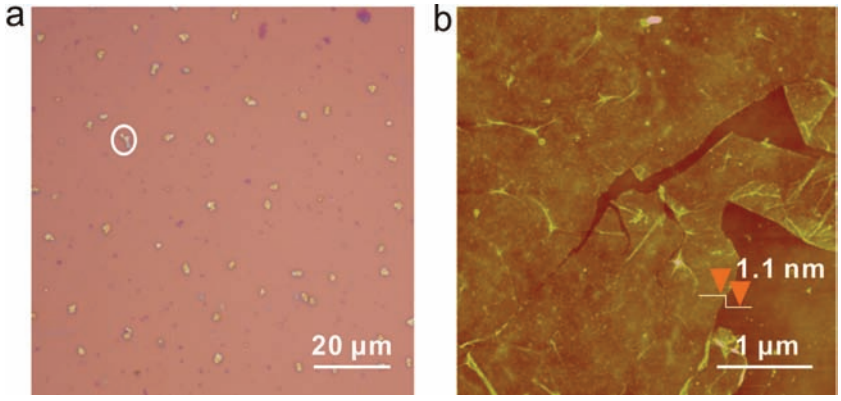

Figure 2. (a) Optical microscope and (b) AFM image of nitrogen-doped graphene on 300 nm-SiO_2/Si substrate. The white circle in the inset of (a) indicates the multilayer area.

to that of G peak, which is consistent with the Raman spectra obtained in electrostatically gated graphene.[13] The 2D to G intensity ratio (I_{2D}/I_G) in NG2 is less than 0.6 (Figure S5), which corresponds to a doping level of >4 × 10^{13} cm^{-2}.[13] Moreover, compared with PG, the G peak of NG2 exhibits a blue shift of 7 cm^{-1}, which is similar to NG synthesized by arc discharge method.[2b,5a] The widths of D, G and 2D peaks in NG are broadened in contrast to PG, which can be ascribed to various bonding structures and defects after doping. The ratio of D to G bands integrated intensities (I_D/I_G) can be used to estimate the crystallite size (L_a) of graphene.[14] We calculated L_a of graphene by the following equation,[6g,15] $L_a(nm) = (2.4 \times 10^{-10})\,\lambda^4 \left(\frac{I_D}{I_G}\right)^{-1}$ where λ is the Raman excitation wavelength (λ = 514.5 nm). The I_D/I_G of PG, NG1 and NG2 are 0.26, 0.80 and 2.1, which correspond to crystallite sizes of 65 nm, 21 nm and 8 nm, respectively. As a consequence, together with the increase of nitrogen doping degree, the crystallite size in NG becomes remarkably decreased as anticipated.

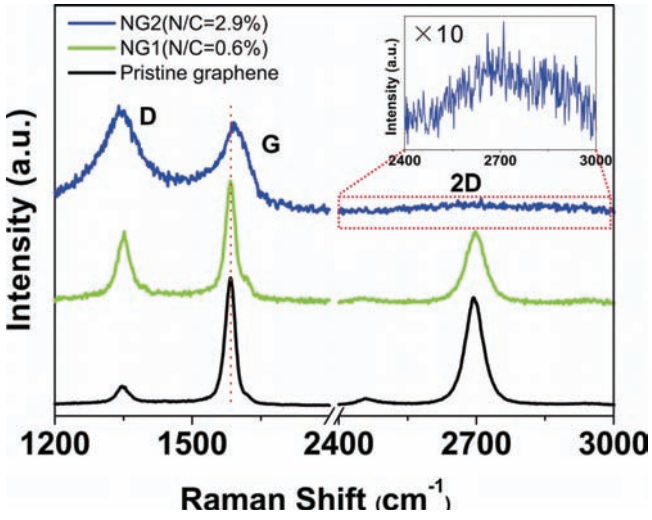

Figure 3. Raman spectra of pristine graphene and nitrogen-doped graphene with low (NG1) and high (NG2) doping concentrations, where D, G and 2D denote the characteristic D band, G band and 2D band of graphene, respectively. The inset shows the enlarged 2D band of NG2. The excitation wavelength is 514.5 nm.

To investigate how N-doping affects the electronic properties of graphene, back-gated field-effect transistors (FETs) of NG and PG were fabricated on 300 nm SiO_2/Si substrates (**Figure 4**a,b). The graphene was cut into strips by photolithography and oxygen plasma etching. As shown in Figure 4a, a typical channel width and length were 30 μm and 80 μm, respectively. To obtain better contact between electrodes and NG/PG, thermal annealing was performed in a reducing (H_2/Ar) atmosphere at 200 °C for one hour. Both NG and PG exhibited p-type characteristics in air (Figures S6, S7c), which could be attributed to the doping by physisorbed molecular oxygen.[6a,6b] To avoid the oxygen doping effect, we measured more than 20 NG devices in vacuum condition (~1 × 10^{-2} Pa) and observed the typical n-type characteristics (Figure 4c,e, S7a,b). Figures 4c and 4d demonstrate the I_{ds}–V_{ds} output characteristics of NG3 (N/C = 1.6 at.%) and PG at variable back-gate voltages (V_g) starting from –60 V to +60 V in a step of 40 V, respectively. The linear I_{ds}–V_{ds} dependence in both cases reveals the good ohmic contact between Au/Cr pads and graphene layer. For PG device, I_{ds} increases with decreasing V_g, indicative of a p-type behavior while for NG device, I_{ds} decreases with decreasing V_g, suggestive of a n-type behavior after nitrogen doping. As is seen in Figure 4e, the Dirac point of NG3 device remarkably shifts to a negative gate voltage in vacuum (~–50 V), demonstrating an n-type electron doping performance. In contrast, the p-type PG device does not show Dirac point at gate voltage from –60 V to +60 V. Moreover, the temperature-dependent electrical transport measurement on a 30-μm-wide NG2 ribbon (Figure 4f) shows a significant resistance increase by more than 80-fold on cooling down from room temperature to 80 K, further demonstrating the semiconducting property of NG sample. The effective bandgap (E_g) of thus-grown NG film can be estimated based on the general relationship, $R(T) \propto \exp(E_g/2k_BT)$, where all the symbols have their common meanings, which is 0.16 eV (see the inset of Figure 4f).

In addition to the ability of growing large-area and uniform NG, our approach is easy to realize selective-area doping by patterning the solid state dopants. For instance, as shown in **Figure 5**a, the nitrogen species were selectively embedded in the right side of the substrate, leading to the half-doping of whole graphene film. There is a clear boundary in optical microscope image, marked by white dotted line in Figure 5a between nitrogen-doping and undoping regions. Figure 5b presents the statistical result of Raman I_{2D}/I_G obtained from two different regions, where the inset shows the typical 2D bands of Raman spectra collected at each side. Obviously, the nitrogen-doped area has a significantly weaker 2D band as compared with the undoped PG area, demonstrating the success of selective area doping of graphene by nitrogen and the formation of NG-PG junction at the boundary.

In summary, we developed a facile technique for growing nitrogen-doped graphene using embedded carbon and nitrogen

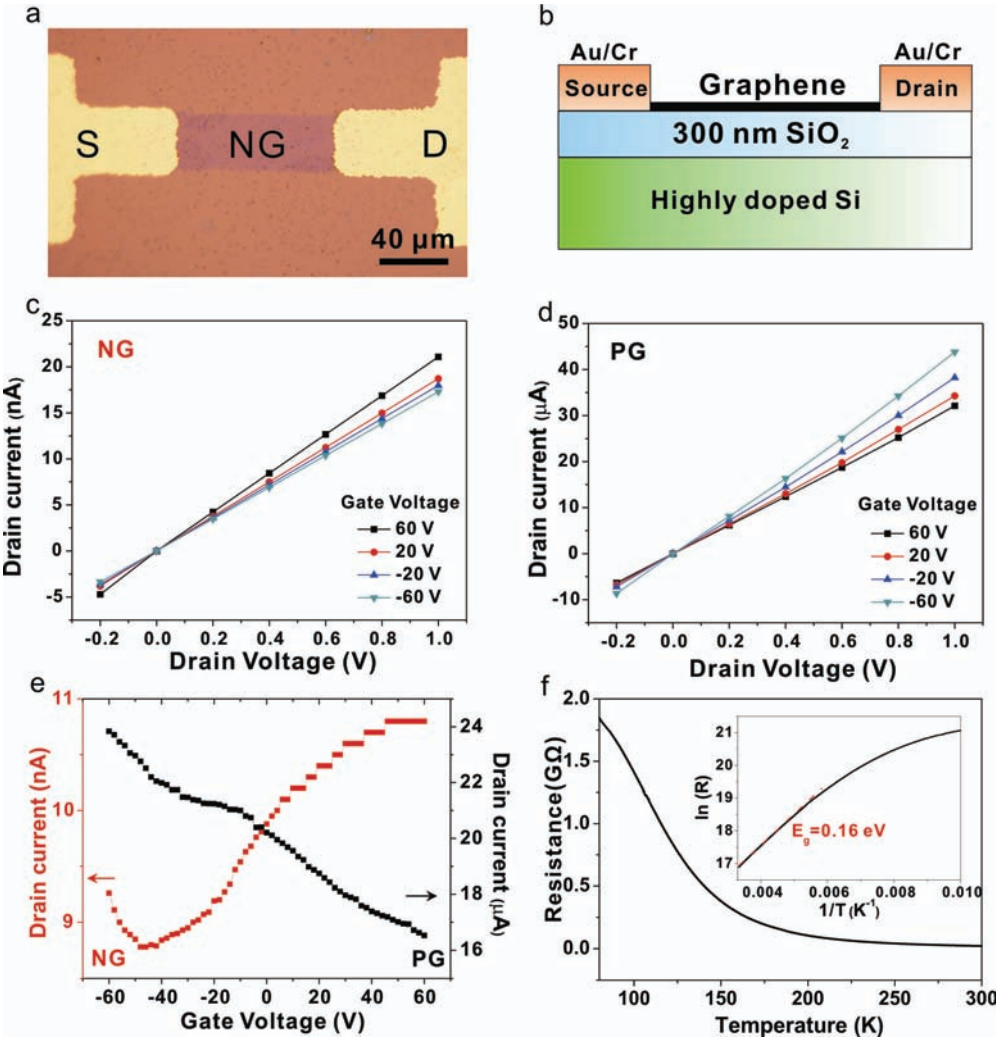

Figure 4. Electrical properties of nitrogen-doped graphene (NG) and pristine graphene (PG) in vacuum. (a) Optical microscope image of NG FET device. (b) Sketch of the device structure. (c) and (d) I_{ds}–V_{ds} output characteristics of NG3 (N/C = 1.6 at.%) and PG at variable back-gate voltages starting from −60 V to 60 V in a step of 40 V, respectively. (e) Transfer characteristics (I_{ds}–V_g) of NG3 (red) and PG (black) devices at V_{ds} = 0.5 V. (f) Temperature dependence of the electrical resistance of NG2 (N/C = 2.9 at.%). The inset shows the change of ln(R) as a function of T^{-1} in the temperature range from 100 to 300 K.

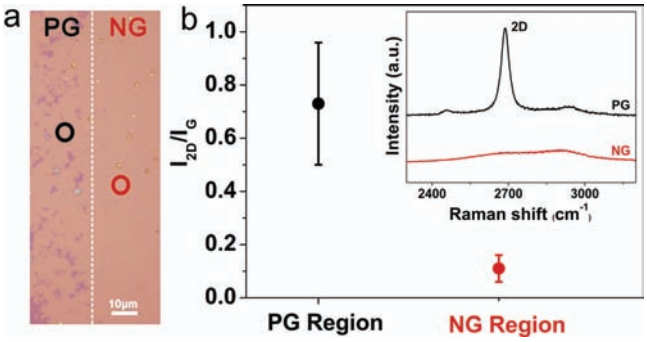

Figure 5. Area-selective doping of graphene. (a) Optical microscope image of the half-doped graphene at boundary region. (b) Statistics of I_{2D}/I_G in the Raman spectra exhibiting the clear difference between undoped (PG, left in (a)) and doped (NG, right in (a)) areas. The inset in (b) shows the corresponding 2D bands of the regions marked in (a).

source. With the enthusiastic utilization of well-known segregation phenomenon, the trace amount of carbon species involved in nickel film as well as the boron-trapped nitrogen species are simultaneously squeezed out via thermal annealing, forming uniform nitrogen-doped graphene film. Compared with pristine graphene, such nitrogen-doped graphene exhibits a remarkable n-type behavior with an effective bandgap of 0.16 eV, suggesting that the nitrogen-doping could tune the electrical properties of graphene. Our method offers the easy control of dopants concentration and location, allowing for the direct growth of pattern-doped graphene and heterojunctions. In principle, it would also be extended to various elements doping of graphene.[16]

Experimental Section

Deposition of boron and nickel films: Boron and nickel films were deposited on SiO_2/Si substrates using electron beam evaporator

(Univex-300, Oerlikon Leybold). The working pressure was maintained at about 2×10^{-3} Pa in the process of electron beam evaporation. The boron and nickel targets (purity higher than 99.9 wt.%) were purchased from General Research of Institute for Nonferrous Metal (GRINM), China. To synthesize nitrogen-doped graphene (NG), we fabricated $Ni/B/SiO_2/Si$ sandwiched substrates: 5–15 nm boron films were evaporated onto a 300 nm thick thermally oxidized silicon wafer at first, followed by depositing 100–300 nm Ni films. For synthesizing pristine graphene (PG), only Ni films were deposited on SiO_2/Si substrate.

Graphene growth: (1) loading samples ($Ni/B/SiO_2/Si$ for NG; $Ni/SiO_2/Si$ for PG) into the vacuum annealing furnace (VTHK-350, Beijing Technol Science Co., Ltd.), evacuating and heating to the desired temperature (800–1100 °C) slowly at a rate of 15–20 °C/min; (2) maintaining the samples at desired temperature for 0–60 min with a pressure of 10^{-3}–10^{-4} Pa; (3) cooling down to room temperature at a rate of 2–50 °C/min.

Transferring graphene to target substrates: Using our nanotransfer-printing method,[11] we can easily isolate thus-grown NG and PG from nickel films and transfer them to arbitrary substrates. A typical transfer-printing procedure includes: (1) spin-coating polymethylmethacrylate (PMMA) film onto graphene-grown substrates ($NG/Ni/B/SiO_2/Si$ or $PG/Ni/SiO_2/Si$); (2) releasing PMMA/graphene film by etching nickel film in $FeCl_3$ solution; (3) putting PMMA/graphene film on target substrates; and (4) dissolving PMMA by acetone.

Characterization: We characterized our samples by optical microscopy (OM, Olympus DX51), atomic force microscopy (AFM, Nanoscope III(a)), Raman spectroscopy (Horiba HR800, with laser excitation at 514.5 nm, 2 mW power), X-ray photoelectron spectroscopy (XPS, AXIS-Ultra), and electrical measurements (Keithley 4200) in air and in vacuum ($\sim 1 \times 10^{-2}$ Pa).

Supporting Information

Supporting Information is available from the Wiley Online Library or from the author.

Acknowledgements

This work was supported by the Natural Science Foundation of China (Grants 50821061, 50802003, 51072004, 20973013, 20833001, 20973006) and the Ministry of Science and Technology of China (Grants 2007CB936203, 2009CB29403, 2011CB933003).

Received: November 7, 2010
Published online: January 14, 2011

[1] a) K. S. Novoselov, A. K. Geim, S. V. Morozov, D. Jiang, Y. Zhang, S. V. Dubonos, I. V. Grigorieva, A. A. Firsov, *Science* **2004**, *306*, 666; b) A. K. Geim, K. S. Novoselov, *Nat. Mater.* **2007**, *6*, 183.

[2] a) D. C. Wei, Y. Q. Liu, Y. Wang, H. L. Zhang, L. P. Huang, G. Yu, *Nano Lett.* **2009**, *9*, 1752; b) L. S. Panchokarla, K. S. Subrahmanyam, S. K. Saha, A. Govindaraj, H. R. Krishnamurthy, U. V. Waghmare, C. N. R. Rao, *Adv. Mater.* **2009**, *21*, 4726.

[3] F. Schwierz, *Nat. Nanotechnol.* **2010**, *5*, 487.

[4] a) L. T. Qu, Y. Liu, J. B. Baek, L. M. Dai, *ACS Nano* **2010**, *4*, 1321; b) A. L. M. Reddy, A. Srivastava, S. R. Gowda, H. Gullapalli, M. Dubey, P. M. Ajayan, *ACS Nano* **2010**, *4*, 6337.

[5] a) K. S. Subrahmanyam, L. S. Panchakarla, A. Govindaraj, C. N. R. Rao, *J. Phys. Chem. C* **2009**, *113*, 4257; b) N. Li, Z. Y. Wang, K. K. Zhao, Z. J. Shi, Z. N. Gu, S. K. Xu, *Carbon* **2010**, *48*, 255.

[6] a) X. R. Wang, X. L. Li, L. Zhang, Y. Yoon, P. K. Weber, H. L. Wang, J. Guo, H. J. Dai, *Science* **2009**, *324*, 768; b) X. L. Li, H. L. Wang, J. T. Robinson, H. Sanchez, G. Diankov, H. J. Dai, *J. Am. Chem. Soc.* **2009**, *131*, 15939; c) Y. Wang, Y. Y. Shao, D. W. Matson, J. H. Li, Y. H. Lin, *ACS Nano* **2010**, *4*, 1790; d) Y. C. Lin, C. Y. Lin, P. W. Chiu, *Appl. Phys. Lett.* **2010**, *96*, 133110; e) R. I. Jafri, N. Rajalakshmi, S. Ramaprabhu, *J. Mater. Chem.* **2010**, *20*, 7114; f) Y. Y. Shao, S. Zhang, M. H. Engelhard, G. S. Li, G. C. Shao, Y. Wang, J. Liu, I. A. Aksay, Y. H. Lin, *J. Mater. Chem.* **2010**, *20*, 7491; g) B. Guo, Q. Liu, E. D. Chen, H. W. Zhu, L. Fang, J. R. Gong, *Nano Lett.* **2010**, *10*, 4975.

[7] a) N. Liu, L. Fu, B. Y. Dai, K. Yan, X. Liu, R. Q. Zhao, Y. F. Zhang, Z. F. Liu, *Nano Lett.*, DOI: 10.1021/nl103962a; b) S. Amini, J. Garay, G. X. Liu, A. A. Balandin, R. Abbaschian, *J. Appl. Phys.* **2010**, *108*, 094321; c) F. Parvizi, D. Teweldebrhan, S. Ghosh, I. Calizo, A. A. Balandin, H. Zhu, R. Abbaschian, *Micro Nano Lett.* **2008**, *3*, 29.

[8] A. J. Pollard, R. R. Nair, S. N. Sabki, C. R. Staddon, L. M. A. Perdigao, C. H. Hsu, J. M. Garfitt, S. Gangopadhyay, H. F. Gleeson, A. K. Geim, P. H. Beton, *J. Phys. Chem. C* **2009**, *113*, 16565.

[9] H. Konno, T. Nakahashi, M. Inagaki, T. Sogabe, *Carbon* **1999**, *37*, 471.

[10] a) J. Xu, M. Saeys, *Chem. Eng. Sci.* **2007**, *62*, 5039; b) J. Xu, M. Saeys, *J. Catal.* **2006**, *242*, 217.

[11] L. Y. Jiao, B. Fan, X. J. Xian, Z. Y. Wu, J. Zhang, Z. F. Liu, *J. Am. Chem. Soc.* **2008**, *130*, 12612.

[12] a) D. Marton, K. J. Boyd, A. H. Al-Bayati, S. S. Todorov, J. W. Rabalais, *Phys. Rev. Lett.* **1994**, *73*, 118; b) S. van Dommele, A. Romero-Izquirdo, R. Brydson, K. P. de Jong, J. H. Bitter, *Carbon* **2008**, *46*, 138; c) J. R. Pels, F. Kapteijn, J. A. Moulijn, Q. Zhu, K. M. Thomas, *Carbon* **1995**, *33*, 1641.

[13] A. Das, S. Pisana, B. Chakraborty, S. Piscanec, S. K. Saha, U. V. Waghmare, K. S. Novoselov, H. R. Krishnamurthy, A. K. Geim, A. C. Ferrari, A. K. Sood, *Nat. Nanotechnol.* **2008**, *3*, 210.

[14] a) D. Teweldebrhan, A. A. Balandin, *Appl. Phys. Lett.* **2009**, *94*, 013101; b) A. C. Ferrari, *Solid State Commun.* **2007**, *143*, 47.

[15] L. G. Cancado, K. Takai, T. Enoki, M. Endo, Y. A. Kim, H. Mizusaki, A. Jorio, L. N. Coelho, R. Magalhaes-Paniago, M. A. Pimenta, *Appl. Phys. Lett.* **2006**, *88*, 163106.

[16] L. J. Ci, L. Song, C. H. Jin, D. Jariwala, D. X. Wu, Y. J. Li, A. Srivastava, Z. F. Wang, K. Storr, L. Balicas, F. Liu, P. M. Ajayan, *Nat. Mater.* **2010**, *9*, 430.